

Regularization of the Solution for Noisy Data Using the FOCUSS Method in Transmission Ultrasound Tomography

Abstract. In the paper, the FOCUSS method was applied to the noisy data, and the effect of the Tikhonov regularization factor on image retrievability was analysed. This method is used to solve systems of underdetermined equations, strongly underdetermined systems could not be solved by this method even with different values of the regularization parameter. It turned out that overdetermined systems can also be solved by this method. The execution time of the algorithm implementing the linear least squares task is much longer than that of the FOCUSS method algorithm.

Streszczenie. W pracy zastosowano metodę fokusową do zaszumionych danych oraz przeanalizowano wpływ współczynnika regularyzacji Tichonowa na odtwarzalność obrazu. Metoda ta służy do rozwiązywania układów równań niezdeteminowanych, silnie niezdeteminowane układy nie mogły być rozwiązane tą metodą nawet przy różnych wartościach parametru regularności. Okazało się, że układy naddeterminowane również mogą być rozwiązywane tą metodą. Czas wykonania algorytmu realizującego zadanie liniowych najmniejszych kwadratów jest znacznie dłuższy od czasu wykonania algorytmu metody FOCUSS (Regularyzacja rozwiązania dla danych zaszumionych przy użyciu metody fokusowej w transmisyjnej tomografii ultradźwiękowej).

Keywords: ultrasound tomography; inverse problem; sensors; FOCUSS method.

Słowa kluczowe: tomografia ultradźwiękowa; problem odwrotny; czujniki; metoda fokusowa.

Introduction

Many optimization methods can be used to solve the inverse in ultrasound tomography [1-9]. The FOCUSS (FOCal Underdetermined System Solver) method [10-12] is used to solve systems of underdetermined linear equations. To introduce the idea of the FOCUSS, the optimization problem associated with solving a system of equations $Ax = b$ by norm minimalization with an additional 'penalty' term is considered. The default form of presumed penalty term is

$$(1) \quad J_p(x) = \sum_{j=1}^n p|x_j|,$$

where $J_p(x)$ is often referred to as multilateral measurement, p is the parameter and x_j are the non-zero values of the matrix x . However, relation (1) can take other forms, e.g.

$$(2) \quad J_p(x) = \text{sign}(p) \sum_{j=1}^n |x_j|^p,$$

where $p \leq 1$ is the chosen parameter. If we want the penalty term to be a measure of Gaussian entropy, then the following applies

$$(3) \quad J_G(x) = H_G(x) = \sum_{j=1}^n \log|x_j|^2.$$

Note that for $p=1$ we obtain a form of linear problem in which at least $n - m$ components are zero. By choosing the factor J_p , we obtain a sparser solution than for the case of a minimum 1-norm solution (corresponding to $p=1$), e.g., for more than $n - m$ zero components in the solution vector. Moreover, the solution may be more accurate in the case of a noisy system. To minimize the solution with a term $J_p(x)$ we define $L(x, \lambda)$ as

$$(4) \quad L(x, \lambda) = J_p(x) + \lambda(b - Wx),$$

where: $\lambda \in \mathbf{R}^n$ is the vector of the Lagrange equation.

We can determine the stationary points of the Lagrange's described above by

$$(5) \quad \nabla_x L(x_*, \lambda_*) = \nabla_x J_p(x) - W^T \lambda_* = 0,$$

$$(6) \quad \nabla_\lambda L(x_*, \lambda_*) = b - Wx_* = 0,$$

where the gradient $\nabla_x J_p(x)$ is expressed as

$$(7) \quad \nabla_x J_p(x) = |p| \mathbf{D}_{|x|}^{-1}(x)x,$$

where $\mathbf{D}_{|x|}(x) \in \mathbf{R}^{(n \times n)}$ is a diagonal matrix with the values of $d_j = |x_j|^{2-p}$. Solving the above equations, we get

$$(8) \quad \lambda_* = |p| (\mathbf{W} \mathbf{D}_{|x|}(x_*) \mathbf{W}^T)^{-1} \mathbf{b},$$

$$(9) \quad x_* = |p|^{-1} \mathbf{D}_{|x|}(x_*) \mathbf{W}^T \lambda_* = \mathbf{D}_{|x|}(x_*) \mathbf{W}^T (\mathbf{W} \mathbf{D}_{|x|}(x_*) \mathbf{W}^T)^{-1} \mathbf{b}.$$

It is recommended that the iterative algorithm for obtaining the optimal vector x_* be given by the formula

$$(10) \quad x(k+1) = \mathbf{D}_{|x|}(k) \mathbf{W}^T (\mathbf{W} \mathbf{D}_{|x|}(k) \mathbf{W}^T)^{-1} \mathbf{b},$$

where $\mathbf{D}_{|x|}(k) = \text{diag}\{x_1^{2-p}(k), x_2^{2-p}(k), \dots, x_n^{2-p}(k)\}$. This algorithm is called FOCUSS and if we denote $\tilde{\mathbf{D}}_{|x|} = \mathbf{D}_{|x|}(k) \mathbf{W}^T$ the formula (10) can be expressed as

$$(11) \quad x(k+1) = \tilde{\mathbf{D}}_{|x|}(k) [\mathbf{W} \tilde{\mathbf{D}}_{|x|}(k)]^+ \mathbf{b},$$

where $[\cdot]^+$ stands for pseudo-inversion according to Moore-Penrose [11,17] and

$$\tilde{\mathbf{D}}_{|x|}(k) = \mathbf{D}_{|x|}^{1/2}(k) = \text{diag}\{x_1^{1-p/2}(k), x_2^{1-p/2}(k), \dots, x_n^{1-p/2}(k)\}$$

The important thing is that the matrix $\mathbf{D}_{|x|}$ exists for all values of x even for negative values of p . For $p=2$, matrix $\mathbf{D}_{|x|} = \mathbf{I}$ (see equation (11) and the FOCUSS algorithm is simplified to a standard least squares task or a 2-norm solution $x_* = \mathbf{W}^T (\mathbf{W} \mathbf{W}^T)^{-1} \mathbf{b}$. In the exceptional case when $p=0$, the diagonal matrix $\tilde{\mathbf{D}}_{|x|} = \text{diag}\{|x_1|, |x_2|, \dots, |x_n|\}$ and instead of using equation (1) we use Gaussian entropy (3), for which the gradient is expressed as:

$$(12) \quad \nabla_x J_G(x) = 2 \mathbf{D}_G^{-1} x,$$

where $\mathbf{D}_G(x) = \text{diag}\{|x_1|^2(k), |x_2|^2(k), \dots, |x_n|^2(k)\}$.

For noisy data, we use the FOCUSS algorithm with a regularization term of the form

$$(13) \quad x(k+1) = \mathbf{D}_{|x|}(k) \mathbf{W}^T (\mathbf{W} \mathbf{D}_{|x|}(k) \mathbf{W}^T + \alpha(k) \mathbf{I})^{-1} \mathbf{b},$$

where $\alpha(k) \geq 0$ is a Tikhonov regularisation parameter [13-15] dependent on the degree of noise.

For systems where there is a multiplication of the tracks of individual sensor systems, the FOCUSS algorithm can be represented as

$$(14) \quad \mathbf{x}(k+1) = \mathbf{D}_{\|\mathbf{x}\|}(k) \mathbf{W}^T (\mathbf{W} \mathbf{D}_{\|\mathbf{x}\|}(k) \mathbf{W}^T)^{-1} \mathbf{b},$$

where: $\mathbf{D}_{\|\mathbf{x}\|}(k) = \text{diag}\{d_1(k), d_2(k), \dots, d_n(k)\}$ and $d_j(k) = \|s_j\|^{2-p}(k)$.

The algorithm can be considered as a standard FOCUSS algorithm described by equation (5) and initialised by using minimum Frobenius solutions. Alternatively, for noisy data, we use the regularisation technique according to Tikhonov or the SVD method with a selection of singular values according to the L-curve principle [14, 16].

Generation methods of the matrix of coefficients

Due to the fact that our considerations concern a circle (cylindrical tube cross-section), therefore, it was necessary to eliminate the pixels that lie outside of the square grid of pixels. A simplification has been adopted consisting in the fact that the circular area will be described with pixels, forming a shape similar to a circle.

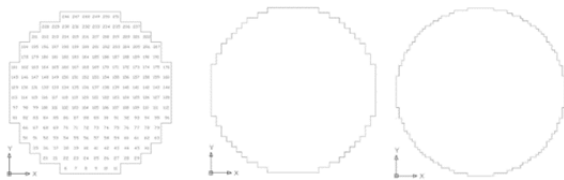


Fig.1. The shape of the area under consideration after applying a square grid a) 16x16, b) 32x32 c) 64x64.

The matrix of coefficients \mathbf{A} from the equation $\mathbf{Ax} = \mathbf{b}$ can be determined in three ways. The first method is the method that can be conventionally called zero-one. Its advantage is simplicity.

The second method, a bit more complicated, replaces the one with the ratio of the length of the passing ray to the diagonal length of the pixel [13]. And the third variant consists in replacing the length of the fields marked by the ray passing through the pixel to the area of the entire pixel. This idea is illustrated in Figures 1 to 4. The zero-one method, the simplest of the methods, consists of the fact that if a ray passes through a given pixel, then in the matrix of coefficients, we put "1" in the appropriate place. In other cases, when the ray does not pass through the pixel, we put "0" into this matrix. Figure 2 illustrates the above principle.

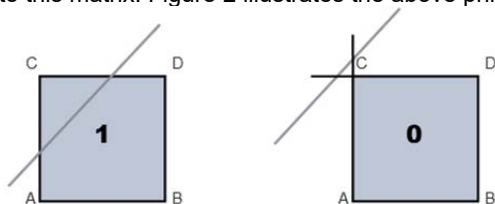


Fig.2. Zero-one rule for determining the elements of the matrix of coefficients.

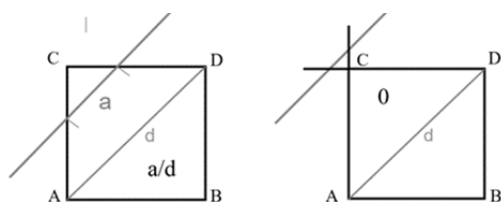


Fig.3. The principle of determining the ratio of the length of a ray running through a pixel to the diagonal length of a pixel.

A modification of this method consists in the fact that instead of inserting ones or zeros, we insert the ratio of the length of the segments: the ray inside the pixel to the diagonal length of the entire pixel. This principle is illustrated in figure 3.

The most advanced modification of the ART method [10], consisting in the fact that we do not put in the appropriate places either 0s or 1s nor the ratio of the length of the ray passing through the pixel to the diagonal of the pixel. Instead, we calculate the ratio of the fields encircled by the ray through the given pixel. The overview drawing is shown below.

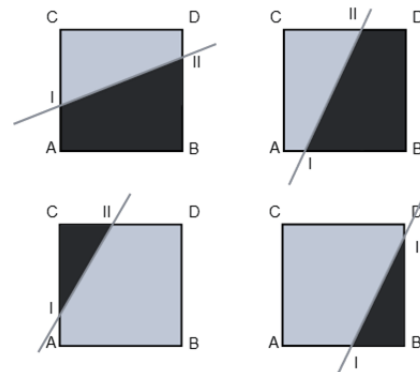


Fig.4. Rays and the fields circled by them.

Having a system constructed in any of these ways of equations, we can proceed to its solution, which is based on the distribution with respect to the singular values of SVD. For this purpose, the Linear Least Squares Problem [14] was used. This method consists in selecting a sample solution for which the result is closest to the model image. This solution was selected on the basis of the graph of the residual vector as a function of the solution vector norm, i.e., the function of the form $\|\mathbf{R}\| = f(\|\mathbf{x}\|)$, where $\mathbf{R} = \mathbf{Ax} - \mathbf{b}$ [14,17]. The best solution is defined as a compromise between the solution that provides the smallest error in the sense of the mean square norm and the solution with the smallest norm i.e., the solution with the smallest oscillations [14].

The method used for solving the system of equations is the FOCUSS method described in detail above.

In order to check the correctness of the algorithm operation, synthetic data was used, i.e., data free of noise and errors. The obtained results were neither filtered nor standardized. These are raw data intended for further processing. Three objects were adopted: square, rectangle and cross. These objects were placed in a circular area with a diameter of 20 cm over which a square grid was placed. In order to reproduce the objects as faithfully as possible, 3 mesh sizes were selected: 16x16 (256 pixels), 32x32 (1024 pixels) and 64x64 (4096 pixels).

The measuring transducers are arranged at equal intervals on the circle, creating eight projection angles, with 8 rays per projection angle, which gives a total of 64 rays. This number, however, turned out to be insufficient for the correct detection of the object, so it was decided to increase their number using the method of linear interpolation. Depending on the resolution of the grid, the following were used: 128, 256, 512, 624, 1024 rays in all eight sensor positions (projection angles).

Results

The figures show images of objects determined with the FOCUSS method: a) reference images, b) c) d) are results for different values of the regularisation parameter. Figures (d) are the results most similar to the reference images.

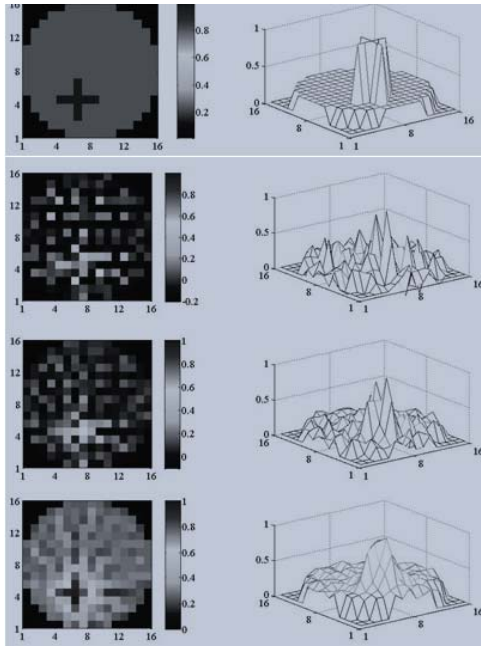


Fig.5. Images of the object with a cross-section at a resolution of 16 by 16 obtained by the FOCUSS method depending on the value of the regularization parameter a) reference image, b) value 0.02, c) value 0.2, d) value 50.

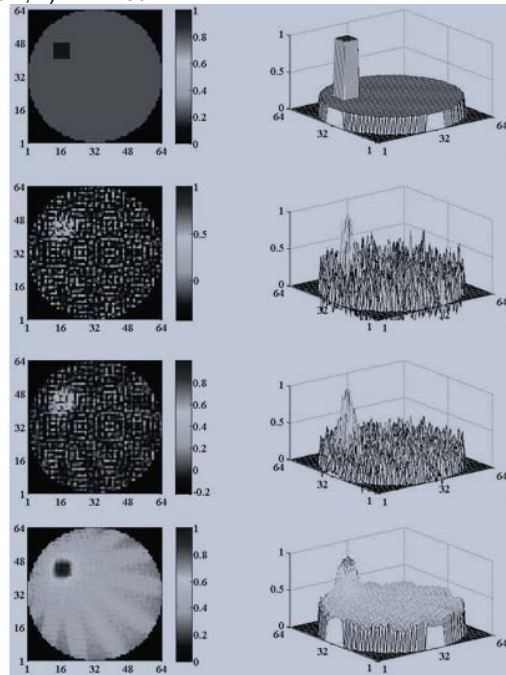


Fig.6. Images of an object with a square cross-section with a resolution of 64 by 64 obtained by the FOCUSS method depending on the value of the regularization parameter a) reference image, b) value 0.02, c) value 0.2, d) value 3.

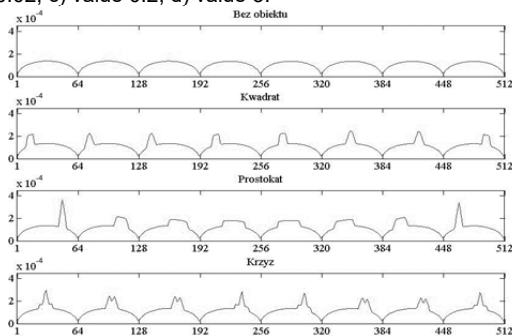


Fig.7. The influence of objects on the transit times of rays in particular orientations: without an object, square, rectangle, cross.

Figure 8 shows images for noise-free data and, at the same time shows the effect of the regularization coefficient on the image.

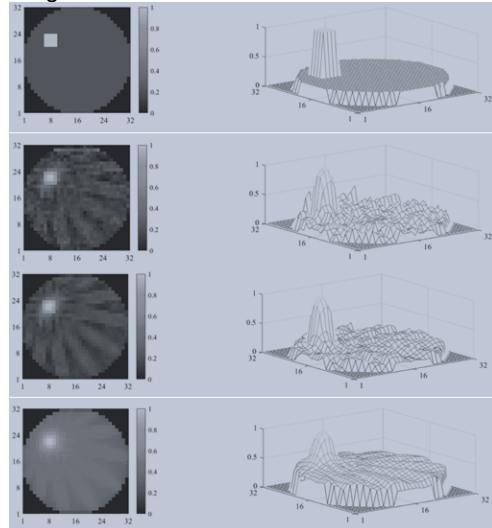


Fig.8. Images of an object with a square cross-section at a resolution of 32 by 32 with 0% noise, obtained by the FOCUSS method depending on the value of the regularization parameter a) reference image, b) value 0.01, c) value 0.2, d) value 15.

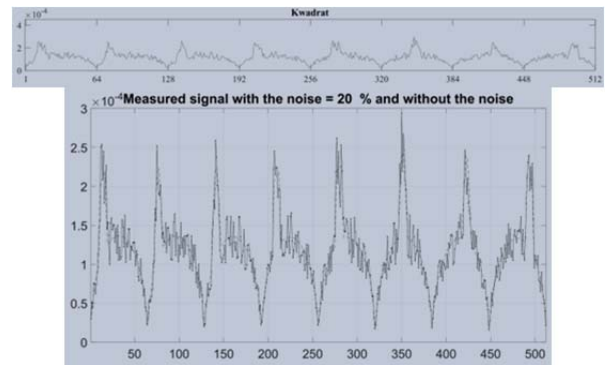


Fig.9. The influence of a square-shaped object on the transit times of rays in particular orientations for 20% of noise; at the bottom of the magnified image - no noise, dashed blue line.

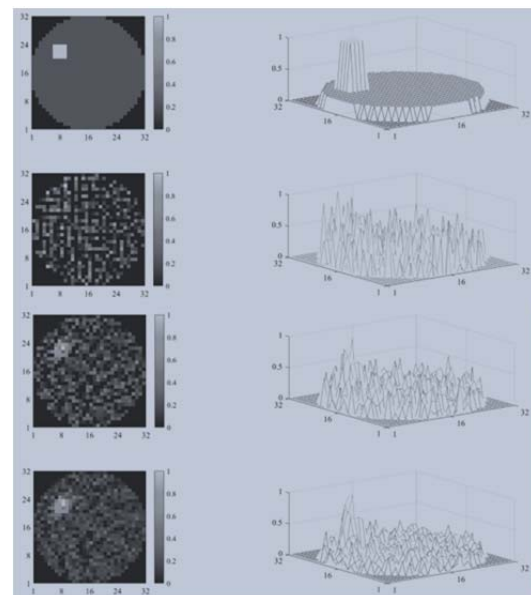


Fig.10. Images of a square object at 32 by 32 resolution with 20% noise, obtained using the FOCUSS method, depending on the value of the regularization parameter a) reference image, b) value 0.0, c) value 0.02, d) value 0.2.

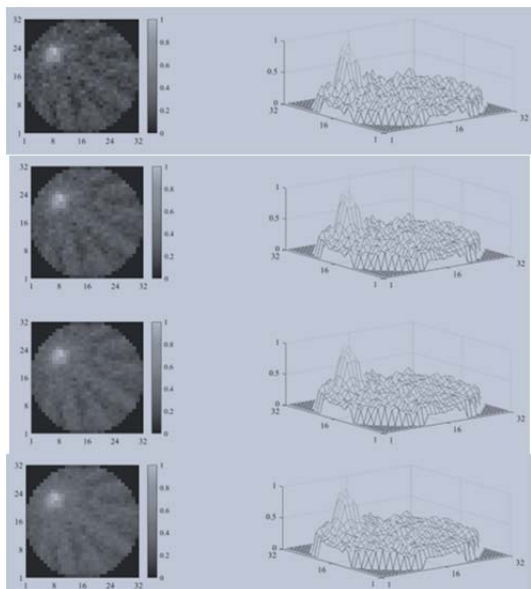


Fig.11. Images of a square object at 32 by 32 resolution with 20% noise, obtained using the FOCUSS method, depending on the value of the regularisation parameter (a) value 2, (b) value 4, (c) value 6, (d) value 8.

Conclusions

When performing the solution of the equation $Ax = b$ by the methods of least squares and FOCUSS, it is possible to observe the differences between them even when the matrix of coefficients A was constructed in the same way (the method of calculating the areas for the 16x16 grid and ART "diagonals" for the 32x32 grid). Although the FOCUSS method is used to solve systems of underdetermined equations, strongly underdetermined systems (such as 64x208, 64x820, 128x820, 64x3224 and 128x3224) could not be solved by this method even with different values of the regularization parameter. However, because of experiments, it turned out that overdetermined systems can also be solved by this method.

The execution time of the algorithm implementing the linear least squares task is much longer than that of the FOCUSS method algorithm. This is due, among other things, to the fact that the Linear Least Squares Problem solution is based on the SVD decomposition of the coefficient matrix A of the system of equations.

Authors: Konrad Kania, M.Sc. Eng., Lublin University of Technology, Nadbystrzycka 38A, Lublin, Poland E-mail: k.kania@pollub.pl; Mariusz Mazurek, Ph.D., Institute of Philosophy and Sociology of the Polish Academy of Science Warsaw, Poland, E-mail: mmazurek@ifispan.edu.pl; Jan Sikora, Netrix S.A/University of Economics and Innovation, Projektowa 4, Lublin, Poland E-mail: sik59@wp.pl.

REFERENCES

- [1] Kłosowski G., Rymarczyk T., Cieplak T., Niderla K., Skowron Ł., Quality Assessment of the Neural Algorithms on the Example of EIT-UST Hybrid Tomography, *Sensors*, 20 (2020), No. 11, 3324.
- [2] Koulountzios P., Rymarczyk T., Soleimani M., A triple-modality ultrasound computed tomography based on full-waveform data for industrial processes, *IEEE Sensors Journal*, 21 (2021), No. 18, 20896-20909.
- [3] Rymarczyk T., Kłosowski G., Hoła A., Sikora J., Wołowiec T., Tchórzewski P., Skowron S., Comparison of Machine Learning Methods in Electrical Tomography for Detecting Moisture in Building Walls, *Energies*, 14 (2021), No. 10, 2777.
- [4] Kłosowski G., Hoła A., Rymarczyk T., Skowron Ł., Wołowiec T., Kowalski M., The Concept of Using LSTM to Detect Moisture in Brick Walls by Means of Electrical Impedance Tomography, *Energies*, 14 (2021), No. 22, 7617.
- [5] Kłosowski G., Rymarczyk T., Kania K., Świć A., Cieplak T., Maintenance of industrial reactors supported by deep learning driven ultrasound tomography, *Eksploracja i Niezawodność – Maintenance and Reliability*; 22 (2020), No 1, 138–147.
- [6] Gnaś, D., Adamkiewicz, P., Indoor localization system using UWB, *Informatyka, Automatyka, Pomiary W Gospodarce I Ochronie Środowiska*, 12 (2022), No. 1, 15-19.
- [7] Styła, M., Adamkiewicz, P., Optimisation of commercial building management processes using user behaviour analysis systems supported by computational intelligence and RTI, *Informatyka, Automatyka, Pomiary W Gospodarce I Ochronie Środowiska*, 12 (2022), No 1, 28-35.
- [8] Korzeniewska, E., Sekulska-Nalewajko, J., Gocawski, J., Drożdż, T., Kiebasa, P., Analysis of changes in fruit tissue after the pulsed electric field treatment using optical coherence tomography, *EPJ Applied Physics*, 91 (2020), No. 3, 30902.
- [9] Korzeniewska, E., Krawczyk, A., Mróz, J., Wysznińska, E., Zawisłak, R., Applications of smart textiles in post-stroke rehabilitation, *Sensors (Switzerland)*, 20 (2020), No. 8, 2370.
- [10] Gorodnitsky I. F., George J. S., Rao B. D., Neuromagnetic source imaging with FOCUSS: a recursive weighted minimum norm algorithm, *Electroencephalogr Clin Neurophysiol*, 95 (1995), 231–251
- [11] Gorodnitsky I. F., Rao B. D., Sparse signal reconstruction from limited data using FOCUSS: a re-weighted minimum norm algorithm. *IEEE Trans Signal Process*, 45 (1997), 600–616
- [12] Polakowski K., Sikora J., Kaczorowski P., Kaźmierczak J., Filipowicz S. F., Liniowe zadanie najmniejszych kwadratów w konstrukcji obrazów wielościeżkowej tomografii ultradźwiękowej, *Przegląd Elektrotechniczny*, 10 (2006), 1824
- [13] Kak C. Avinash, Slaney Malcolm: Principles of Computerized Tomographic Imaging, The Institute of Electrical and Electronics Engineers, Inc. New York, 1988
- [14] Lawson Ch.L., Hanson R.J., Solving Least Squares Problems, *Classics in Applied Mathematics*, 15 (1995), SIAM
- [15] Rymarczyk T., Tomographic Imaging in Environmental, Industrial and Medical Applications, Innovation Press Publishing House, 2019
- [16] Opieliński J. K., Analiza możliwości zobrazowania struktury wewnętrznej obiektów metodą ultradźwiękowej tomografii transmisyjnej, Praca doktorska, Wrocław 1998
- [17] Rymarczyk T., Sikora J., Polakowski K., Adamkiewicz P., Efektywny algorytm obrazowania w tomografii ultradźwiękowej i radiowej dla zagadnień dwuwymiarowych, *Przegląd Elektrotechniczny*, 94 (2018).